

# We are IntechOpen, the world's leading publisher of Open Access books Built by scientists, for scientists

4,800

Open access books available

122,000

International authors and editors

135M

Downloads

Our authors are among the

154

Countries delivered to

TOP 1%

most cited scientists

12.2%

Contributors from top 500 universities



WEB OF SCIENCE™

Selection of our books indexed in the Book Citation Index  
in Web of Science™ Core Collection (BKCI)

Interested in publishing with us?  
Contact [book.department@intechopen.com](mailto:book.department@intechopen.com)

Numbers displayed above are based on latest data collected.  
For more information visit [www.intechopen.com](http://www.intechopen.com)



# Developing Functionality in Perovskites from Abatement of Pollutants to Sustainable Energy Conversion and Storage

*Andrea Bedon and Antonella Glisenti*

## Abstract

Different functionalities can be developed and optimised in perovskites by means of different approaches: doping, nanocomposition and exsolution. In our research, these strategies are used with the aim of a sustainable development. Our objectives are in developing perovskite-based materials for catalysis and electrocatalysis. In particular, we successfully obtained catalysts for abatement of pollutants in three-way catalysts, catalysts for dry reforming of methane and electrocatalysts for solid oxide cells (solid oxide fuel cells and solid oxide electrolyzers). In all cases, the corresponding device and experimental set-up was optimised. The catalysts and electrocatalysts we considered are free of noble metals and with minimum amount of critical raw materials. The preparation procedures are by wet chemistry, highly reproducible and up-scalable.

**Keywords:** catalysis, electrocatalysis, nanocomposition, doping, oxygen exchange, solid oxide cells, three-way catalysts, sustainable development, energy storage and conversion, pollutants abatement

## 1. Introduction

Several materials and devices are very efficient in terms of catalytic and electrocatalytic performance because of the presence of noble metals. Due to the cost and difficulty of supply, the European Community decided that the minimization of noble metals use is a fundamental step for economic and social development. Perovskites are good candidates for substituting noble metals in devices because of their versatility and low economic and environmental impact. The perovskites we focus on are oxides of the type  $ABO_3$  (with A = alkali or alkali earth or rare earth and B = transition metal, usually) [1]. These are very stable oxides, characterised by great versatility in composition, tolerance to structural deformation and, typically, low cost. The functionality of perovskites can be enhanced using different approaches. In this chapter, several strategies for the enhancement of catalytic and electrocatalytic performance are described and compared. Numerous devices require materials characterised by similar properties such as the capability to dissociatively coordinate molecules, the ionic mobility and exchange capability, the thermal and morphological stability, etc. Different methodologies allow to build

functionality in perovskite-type oxides; among these, doping, nanocomposition and exosolution are the more relevant, being more easy to control and characterised by higher effect. The doping in A-site is fundamental to affect the oxygen mobility and ion conductivity but can also enforce a redox couple. The deformation caused by this doping may have relevant effects on electronic conductivity and mobility. Doping in B-site is a precious help in creating redox behaviour and, consequently, catalytic activity and electronic conductivity. When different properties are required, it can be easier to model the behaviour through nanocomposition. The synergy between supported and supporting phases, in fact, allows obtaining higher performances when compared to the sum of the two. At this purpose, several aspects are relevant in affecting the behaviour of the interfaces and they will be considered. The rearrangement of perovskite surface is very relevant in determining the interaction between molecules (reactants, intermediates and products), and exosolution can be very effective in inducing the reconstruction of active surfaces.

These procedures for enhancing and tuning the catalytic and electro-catalytic performances of perovskite-based material will be compared and evaluated taking into consideration three applications and devices: solid oxide cells (fuel cells—SOFCs—and electrolyzers—SOECs), catalysis for abatement of pollutants (three-way catalysts, TWC) and for green hydrogen/green fuel generation (dry reforming of methane, DRM).

## 2. Developing functionality in perovskites for a sustainable development: experimental

### 2.1 Synthesis

The samples are always prepared by citrate method [2] starting from a solution of precursors to which citric acid is added. The molar ratio of citric acid

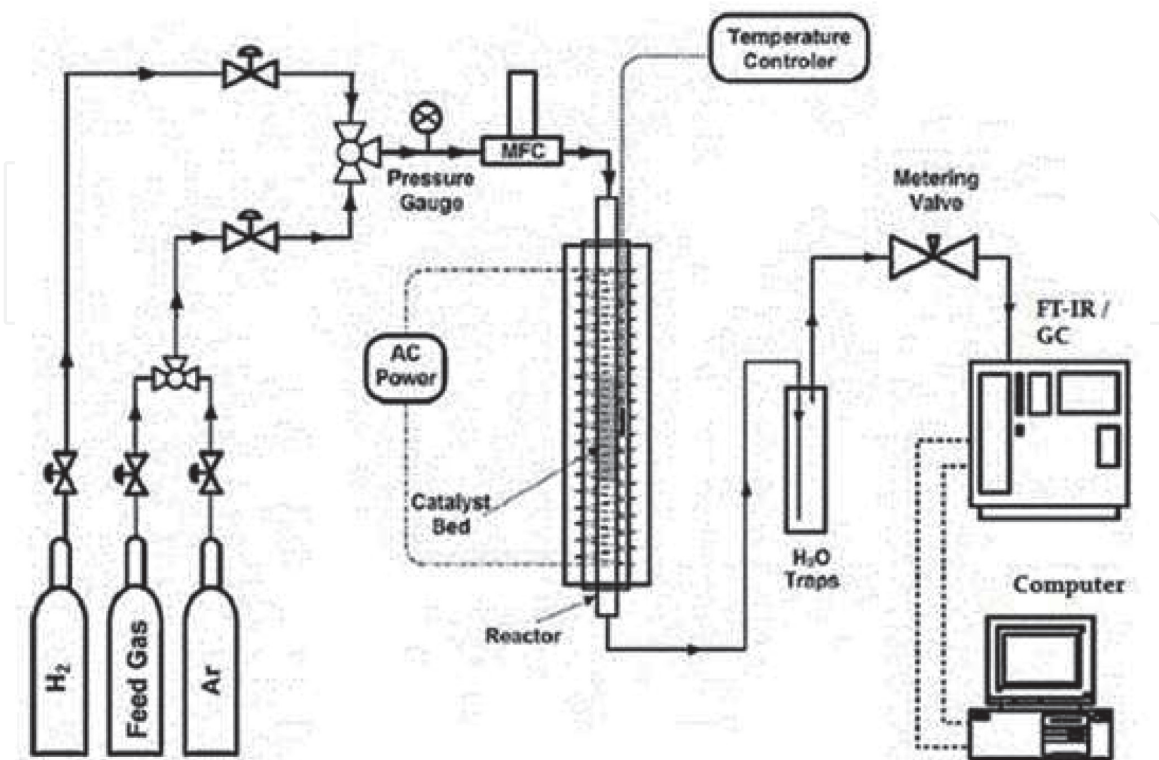


**Figure 1.**  
*Experimental set-up used for the catalytic activity measurements.*

monohydrate was 1.9:1 with respect to the total amount of cations. Then the solution is heated up to 90°C in air to promote water evaporation and to obtain a wet gel. The gel is treated up to 400°C for 2 h in air to decompose the organic framework, and the obtained powder samples were grinded and calcined at the appropriate temperature in air or in reducing atmosphere depending on the required phase.

Impregnation [3] is a process commonly used to enhance the performances of a material, and consists in depositing a new phase on an existing substrate from a solution. Wet impregnation is the more common and traditional procedure that allows depositing the required amount of active phase; where in incipient wetness, the deposited quantity is strictly related to the solubility of precursors [4]. In wet impregnation, it is sometimes difficult to reach high dispersion and is thus necessary to develop new procedures. The strategy we followed consists in depositing the precursor in complexed form so to favour the interaction with the supporting surface and limit particles coalescence.

## 2.2 Characterisation

The XPS measurements were carried out (with a Perkin Elmer  $\Phi$  5600ci multi-technique system) to evaluate surface composition both in terms of oxidation state of the composing elements and of quantitative analysis. At this purpose, it is interesting to compare the XPS results with EDX ones, which consider a deeper layer. Field emission scanning electron microscopy and EDX measures (around at. % accuracy) were carried on a Zeiss SUPRA 40VP. Morphological analysis and EDX analysis were carried out setting the acceleration voltages at 20 kV.

The XRD analyses were performed with a Bruker D8 Advance diffractometer with Bragg-Brentano geometry using a Cu K $\alpha$  radiation (40 kV, 40 mA,  $\lambda = 0.154$  nm). The data were collected at 0.03° at a counting time of 7 s/step in the (2 $\theta$ ) range from 20 to 70°. The crystalline phases were identified by the search-match method using the JCPDS database; the position of the peaks, furthermore, allows to evaluate, on the base of the crystal unit cell parameters, the inclusion of the dopant inside the perovskite cell. Temperature-programmed reduction (TPR) and specific surface area (BET) measurements were performed with an Autochem II 2920 Micromeritics, equipped with a TCD detector. The TPR measurements were carried out in a quartz reactor by using 50 of sample and heating from RT to 900°C at 10°C min<sup>-1</sup> under a constant flow of H<sub>2</sub> 5% in Ar (50 ml • min<sup>-1</sup>). TPR samples were previously outgassed with He (50 ml • min<sup>-1</sup>) at RT. The critical evaluation of the XPS and TPR data on oxidation state of cations can be very useful because TPR is a bulk quantitative analysis that considers the whole powder while XPS is surface specific one. The comparison between XPS and TPR data allows to understand segregation phenomena and to individuate the first sites responsible of the reactivity and also to evaluate the exchange and bulk intervention. In BET measurements, 100 mg of sample was used; before measurement, the sample was treated at 350°C for 2 h under a constant flow of He (50 ml • min<sup>-1</sup>); each surface area obtained was the average of three consecutive measurements. Temperature-programmed desorption (TPD) measurements were performed with an Autochem II 2920 Micromeritics, equipped with a TCD detector and whose outlet was directly connected with a quadrupole mass spectrometer (QMS, ESS Genesis). The TPD measurements were carried out in a quartz reactor by using approximately 0.1 grams of perovskite powder. The data were collected under a constant flow of Helium. O<sub>2</sub>-temperature-programmed desorption (TPD) measurements were carried out after a treatment with O<sub>2</sub> at 650 (for LaCoO<sub>3</sub>) and 600°C (for the doped LaCoO<sub>3</sub>). The O<sub>2</sub>-TPD measurements allow to study the effect of composition and doping on the formation and stabilization of  $\alpha$ - and  $\beta$ -oxygen species and thus on oxygen ions mobility and on surface and bulk oxygen vacancies.



### 2.3 Catalytic activity

The catalytic activity tests were carried out, at atmospheric pressure, under different conditions depending on the specific reaction and application. Measurements were carried out in a quartz reactor (6 mm ID) with a packed bed of powders (**Figure 1**); the temperature was monitored by a thermocouple right upstream of the bed reactor. The experimental set-up has been already described [5].

Soot oxidation tests were conducted both in tight and loose contact mode [6] using a 1:10 soot to catalyst ration, in a 5% O<sub>2</sub> atmosphere. In this case, the inert carrier used was He, and the temperature of the catalytic bed was raised from RT until no production of CO<sub>2</sub> could be detected.

The composition of the gas mixture (before and after reaction) was measured by GC (Agilent 7890A), with a TCD detector.

### 2.4 Electrocatalytic activity

Electrochemical behaviour was studied by means of impedance spectroscopy tests performed on symmetric or asymmetric cells (to evaluate the electrode or the whole device). Impedance of the cell was measured under air (normal operating



**Figure 2.**  
*Image of the experimental equipment for the test of the solid oxide cells.*

condition for a SOFC cathode or SOEC anode) and in presence of fuel ( $H_2$ ,  $CH_4$ ). The home-made equipment is reported in **Figure 2** and is connected with an Autolab Metrohm PGSTAT204.

### 3. Developing functionality in perovskites for a sustainable development: results and discussion

#### 3.1 Cases of built functionality: the art of pollutants abatement

##### 3.1.1 Making a poorly active perovskite active in CO oxidation and NO reduction: the difficult case of $SrTiO_3$

$SrTiO_3$  is a very robust perovskite composed by very cheap, not critical and environmentally sustainable elements. Unfortunately, its catalytic activity is rather low and this compound is neither active in CO oxidation nor in NO reduction. An interesting improvement can be represented by the introduction of a redox couple in the B-site. This result can be obtained by both substituting Sr with an alkaline earth and introducing a transition metal in the B-site. Co and Mn are mostly the more active cations in oxidation; so these cations have been our first choice. In perovskite doping, the improvement of the properties (oxygen exchange and mobility, catalytic activity, etc.) derives from the insertion of dopant into the unit cell. To reach this goal, a particular care has to be devoted to evaluate the solubility and the optimal doping amount. Several attempts convinced us that a good composition could be for cobalt doping,  $SrTi_{0.7}Co_{0.3}O_3$ . The insertion was confirmed by the characterisation (particularly XRD and TPR). The inclusion of cobalt induces the formation of a redox couple and of oxygen vacancies that are responsible of the increased catalytic activity with respect to CO oxidation (**Table 1**). A similar attempt was carried out with Cu with the aim of increasing the catalytic activity in NO reduction. This doping, however, did not result to be of any help. In fact, no significant signal due to Cu(II) reduction is observed suggesting that once inserted into the crystalline cell, copper loses its reducibility. Usually, the reduction of copper follows its diffusion toward the perovskite surface, so we can suppose that mobility is un-favored in this case [7–12].

To take, however, advantage of the presence of copper, nanoparticles of CuO were deposited onto the surface of  $SrTi_{0.7}Co_{0.3}O_3$  by wet impregnation. This allowed to add the reactivity towards NO reduction due to the copper nanoparticles and to the reactivity towards CO oxidation due to Co-doped perovskite.

Temperature °C	$SrTi_{0.7}Co_{0.3}O_3$		$CuO/SrTi_{0.7}Co_{0.3}O_3$	
	CO oxidation	CO + NO	CO oxidation	CO + NO
	CO Conversion	NO conversion	CO Conversion	NO conversion
100	0	0	0	0
200	19	0	2	8
300	84	0	43	43
350	91	0	68	100
400	90	0	79	100

**Table 1.** Conversion values obtained, at different temperature, on the Co-doped  $SrTiO_3$  and in the nanocomposite  $CuO/SrTi_{0.7}Co_{0.3}O_3$  obtained by wet impregnation.

In the nanocomposite, the activity in CO assisted NO reduction greatly increases (**Table 1**) while that in CO oxidation does not decrease significantly.

SrTiO<sub>3</sub> was also activated with a different strategy consisting in doping both in Sr- and Ti-sites. For Sr-site, the substitution with K was attempted, whereas for the Ti-site, Mn was preferred. We expected that both oxygen vacancies formation and Mn-based redox couples could form and be precious in enhancing the catalytic activity [13]. This hypothesis was confirmed by the experimental data (**Table 2**). In the undoped SrTiO<sub>3</sub>, no activity was observed. When Mn is added, the conversion in CO oxidation increases from 18 to 94% at 600°C. The best performance for CO assisted NO reduction is observed when a composite is obtained by depositing CuO on K and Mn-doped SrTiO<sub>3</sub>.

Also the soot oxidation is improved by doping in the Sr-site and Ti-site (**Table 3**).

### 3.1.2 Copper activation: inside the perovskite cell or deposited onto the surface?

The behaviour of dopants and the capability to improve the reactivity depend on the specific perovskite and can be discussed in terms of structural and chemical stabilization. The insertion of copper as a substitute of cobalt in a LaCoO<sub>3</sub> perovskite, as an example, greatly increases the reactivity of undoped perovskite with

	Reaction	Temperature (°C)	Conversion CO	Conversion NO	Conversion CO
SKT	CO + O <sub>2</sub>	400	0		
	CO + O <sub>2</sub>	600	18		
	CO + NO	400		2	5
	CO + NO	600		5	10
SKTM <sub>30</sub>	CO + O <sub>2</sub>	400	54		
	CO + O <sub>2</sub>	600	94		
	CO + NO	400		25	25
	CO + NO	600		50	49
Cu/SKTM <sub>30</sub>	CO + NO	400		100	94
	CO + NO	600		100	100

**Table 2.**

Conversion values obtained at 400 and 600°C for the K-doped, K and Mn-doped SrTiO<sub>3</sub> (Sr<sub>0.8</sub>K<sub>0.2</sub>TiO<sub>3</sub>, SKT—Sr<sub>0.8</sub>K<sub>0.2</sub>Ti<sub>0.7</sub>Mn<sub>0.3</sub>O<sub>3</sub>—SKTM<sub>30</sub>) and for a nanocomposite obtained by depositing CuO on Mn-doped SrTiO<sub>3</sub> (Cu/SKTM<sub>30</sub>).

Catalyst	T <sub>onset</sub>	T <sub>max</sub>	CO <sub>2</sub> conversion
SKT	307	346	89
SKTM <sub>15</sub>	276	333	89
SKTM <sub>30</sub>	261	329	89
SKTM <sub>30</sub> 800	264	327	81

**Table 3.**

Onset temperature and temperature of maximum conversion of soot in presence of 10% O<sub>2</sub> and with a soot: catalyst of 1:10. The amount of converted CO<sub>2</sub> with respect to the total expected CO<sub>2</sub> is also reported (Sr<sub>0.8</sub>K<sub>0.2</sub>TiO<sub>3</sub>, SKT—Sr<sub>0.8</sub>K<sub>0.2</sub>Ti<sub>0.85</sub>Mn<sub>0.15</sub>O<sub>3</sub>—SKTM<sub>15</sub>; Sr<sub>0.8</sub>K<sub>0.2</sub>Ti<sub>0.7</sub>Mn<sub>0.3</sub>O<sub>3</sub>—SKTM<sub>30</sub>). All samples are treated at 700°C calcination temperature; the effect of increasing the calcination temperature is reported comparing SKTM<sub>30</sub> (treated at 700°C) and SKTM<sub>30</sub> 800 (treated at 800°C).

respect to the NO reduction. Several aspects contribute to this result. The first copper insertion into the lattice causes the formation of oxygen vacancies for electroneutrality reasons. The NO molecules interact dissociatively with the surface oxygen vacancies that, in this way, play a key role in NO activation (usually the rate determining step). CO can interact with the Lewis active sites distributed on the surface (Co cations, as an example), which is the first step for its oxidation [14, 15].

Doping can also increase the oxygen mobility and exchange capability, which is fundamental for oxidation, considering the Mars-van-Krevelen mechanism; in fact, the capability of perovskite to oxidize CO is fundamental.

The effect of doping with Cu was investigated by our research group and compared with the case of Cu deposited on LaCoO<sub>3</sub> (Tables 4 and 5, Figure 3).

Copper inside the perovskite cell, as mentioned, increases the reactivity thanks to the formation of oxygen vacancies activating small molecules but under oxidizing environment, it is difficult for oxygen vacancies to survive on surface and thus the activating effect of copper is due to the capability of this cation to coordinate more than one NO molecule facilitating the formation of the N<sub>2</sub>O intermediate that evolves into the formation of N<sub>2</sub> and O<sub>2</sub>.

At high Cu/Co atomic ratios, there is no significant difference between the two synthetic approaches, but with lower Cu contents, the nanocomposites seem more active in CO oxidation. A complex situation is observed in NO reduction: at lower Cu/Co atomic ratios, the LaCo<sub>1-x</sub>Cu<sub>x</sub>O<sub>3</sub> catalysts are more active than the nanocomposites. This suggests that the surface is mainly involved in the NO

Temperature	Reaction	x = 0	x = 10	x = 15	x = 20	x = 30	x = 15 WI
200	CO + O <sub>2</sub>	80	7	75	69	73	4
	CO+ NO	0	2 (1)	0 (0)	0 (0)	0 (0)	0 (0)
250	CO + O <sub>2</sub>	92	87	88	85	90	73
	CO+ NO	0	6 (3)	4 (5)	4 (0)	0 (0)	0 (0)
300	CO + O <sub>2</sub>	94	91	93	92	93	85
	CO+ NO	0	18 (17)	62 (56)	67 (59)	42 (36)	6 (5)
350	CO + O <sub>2</sub>	96	94	94	94	97	94
	CO+ NO	2 (1)	39 (36)	80 (71)	81 (66)	94 (76)	68 (63)
400	CO + O <sub>2</sub>	100	100	100	100	100	100
	CO+ NO	4 (2)	100 (92)	100 (92)	97 (92)	100 (92)	83 (77)

**Table 4.** Conversion values obtained, at different temperature, on the xCuO/LaCoO<sub>3</sub> with x = atomic percentage.

Temperature	Reaction	0	0.1	0.3	0.5
200	CO + O <sub>2</sub>	80	5	2	94
	CO+ NO	0	0 (3)	13 (0)	0 (2)
250	CO + O <sub>2</sub>	92	24	46	93
	CO+ NO	0	8 (2)	11 (23)	45 (42)
300	CO + O <sub>2</sub>	94	66	67	96
	CO+ NO	0	8 (7)	24 (25)	63 (58)
350	CO + O <sub>2</sub>	96	86	79	96
	CO+ NO	2 (1)	52 (45)	80 (72)	83 (70)
400	CO + O <sub>2</sub>	100	94	95	96
	CO+ NO	4 (2)	71 (77)	100 (95)	97 (95)

**Table 5.** Conversion values obtained, at different temperature, on the doped perovskite LaCo<sub>1-x</sub>Cu<sub>x</sub>O<sub>3</sub>.



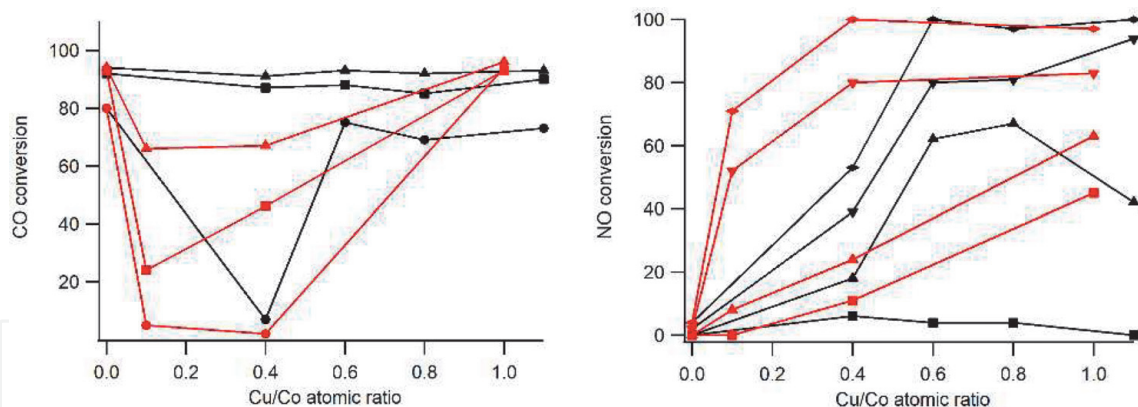


**Figure 3.** (Left) CO conversion (in CO oxidation) and (right) NO conversion (in CO + NO) observed as a function of the Cu/Co atomic ratio for the catalysts with copper inside the cell (red) and deposited on the  $\text{LaCoO}_3$  surface (black).  $\bullet$  200°C,  $\blacksquare$  250°C,  $\blacktriangle$  300°C,  $\blacktriangledown$  350°C and  $\blacklozenge$  400°C.

activation by means of oxygen vacancies until Cu content is high enough to favour another mechanism, frequently observed in simple oxides that, unlike perovskites, are not characterised by the presence of oxygen vacancies. Following this mechanism, NO molecules are activated by coordination to the Cu clusters.

Other nanocomposites can behave in a different way: in the soot oxidation carried out with  $\text{LaMnO}_3$ -based perovskites, as an example. To enhance the activity in oxidation, we doped substituting Mn with Co. Co oxides are very active catalyst for oxidation [16] but the use of cobalt is not very easy from an industrial point of view. So we decided to use this element as a dopant of Mn. In this case, we used K as a dopant in the A-site in the attempt to oxidize soot comparing with the effect of depositing K oxide on the surface of the perovskite. It is evident from the temperature of maximum conversion (**Table 6**) that the better result (lower maximum activity temperature,  $T_{\text{max}}$ ) is obtained when La is used as a 12-coordinated cation (pushing manganese to be Mn(III)) and K is inserted into the perovskite unit cell.

Also the doping in the A-site is a powerful mean to increase the reactivity [17]. In this case, the aliovalent substitution of La with an alkali earth or an alkaline element determines both the formation of the oxygen vacancies and the increment of the oxidation state of the cation in the B-site. As an example, in the  $\text{LaCoO}_3$ , the substitution with Sr can favour also the formation of Co in unusual oxidation state as IV but the low stability of this specie suggests also the formation of oxygen vacancies. The equilibrium between these two effects of doping depends on the redox potential, the strength of the M-O bonds, etc. allowing for the creation of several different and complementary reaction mechanisms whose relevance depends also on temperature. In  $\text{LaCoO}_3$ -based catalysts, as an example, around 350°C, the CO oxidation mechanism changes from suprafacial to intrafacial; pulsed

Sample	$T_{\text{max}}$
Only soot—no catalyst	627
$\text{LaMn}_{0.9}\text{Co}_{0.1}\text{O}_3$	330
$\text{La}_{0.9}\text{K}_{0.1}\text{Mn}_{0.9}\text{Co}_{0.1}\text{O}_3$	306
$\text{Sr}_{0.9}\text{K}_{0.1}\text{Mn}_{0.9}\text{Co}_{0.1}\text{O}_3$	323
0.1 K/ $\text{LaMn}_{0.9}\text{Co}_{0.1}\text{O}_3$	330

**Table 6.** Temperature of maximum activity in soot oxidation (10%  $\text{O}_2$  + 5000 ppm NO) for different  $\text{LaMnO}_3$ -based catalysts.

Sample	Reaction	200°C	250°C	300°C	350°C	400 °C
LaCoO <sub>3</sub>	MSR	0	0	0	0	0
	ESR	0	0	0	0	7
	MOSR	2	15	28	13	24
	EOSR	1	11	12	41	37
LaCo <sub>0.7</sub> Cu <sub>0.3</sub> O <sub>3</sub>	MSR	0	30	50	67	80
	ESR	4	24	28	20	24
	MOSR	0	6	51	84	90
	EOSR	1	12	43	70	77
La <sub>0.7</sub> Sr <sub>0.3</sub> CuO <sub>3</sub>	MSR	0	3	12	18	14
	ESR	0	7	48	68	35
	MOSR	0	7	9	99	100
	EOSR	0	3	8	21	100

**Table 7.**

Conversion obtained in un-doped and doped LaCoO<sub>3</sub> in methanol steam reforming (MSR), ethanol steam reforming (ESR), methanol oxidative steam reforming (MOSR) and ethanol oxidative steam reforming (EOSR).

experiments optimised for perovskites allowed to evaluate that the activation energy decreases from 40 (for undoped) to 29 (Sr-doped) to 27 (Cu-doped) kJ/mol [18]. Doping can have a different effect on the activity and selectivity being, these properties, related to different properties of the catalysts. The substitution of La with Sr increases the activity in NO reduction, when a complex mixture simulating the automotive exhaust is used, but not for the CO assisted NO reduction [17].

In LaMnO<sub>3</sub>, the formation of oxygen vacancies is, in contrast, less favoured with respect to that of Mn(IV) which is a stable state for manganese; so the catalytic properties can be tuned in a different way.

So depending on the required catalytic activity, different dopants and different reactions can be enhanced. A similar strategy can be successfully applied to processes different from abatement of pollutants. A lot of relevance, as an example, is gathered by the steam reforming and oxidative steam reforming of alcohol. Also in this case, the doping with copper greatly improves the activity of LaCoO<sub>3</sub> both in ethanol and even more in methanol steam reforming and oxidative steam reforming. The results are surely due to the presence of copper, as demonstrated by the activity and selectivity of a LaSrCuO<sub>3</sub> in methanol and ethanol steam reforming and oxidative steam reforming (**Table 7**) [19, 20].

### 3.1.3 NO<sub>x</sub> reduction: a very difficult challenge. Improvements derived from smart nanocomposition

The reactivity developed in perovskite-based nanocomposites is strongly dependent on the supporting perovskite and on the interaction of the surface with the deposited phase. In particular, it is widely accepted that higher performance can be obtained through high dispersion of activating particles. With the aim of a deeper understanding, traditional wet impregnation and an innovative ammonia driven precipitation procedure were compared in terms of dispersion (by means of TPR) and catalytic activity. Both model reactions (CO oxidation and CO assisted NO reduction) and reactions with a synthetic automotive exhaust mixture, including 10% steam, and oxygen, were carried out. The catalytic results clearly underline that higher dispersion means higher catalytic activity and that the difference is particularly evident at lower temperature. To favour the dispersion of nanoparticles, the interaction at the interface is paramount. A strong interaction prevents the particles sintering and allows to expose a higher amount of active sites.

It has to be considered that some molecules are activated at the interface steps where coordinatively unsaturated sites are more accessible [15, 21, 22].

A good choice of the support (that can be characterised by a specific reactivity) and of the activating nanoparticles allows to build an interesting reactivity. In our work, we compared the deposition of copper oxide carried out on  $\text{LaCoO}_3$  and  $\text{LaNiO}_3$ . In both cases, the nanocomposites show good activity in oxidation and in NO reduction, with performance greatly enhanced with respect to the single components, but in the  $\text{CuO}/\text{LaNiO}_3$  case, the activity in NO reduction is increased thanks to the presence of  $\text{H}_2$  that originates from the steam reforming catalyzed by the support; so, a successful synergic approach is obtained.

We compared the results with the ones obtained in similar reactions with  $\text{CuO}/\text{LaCoO}_3$ . Different interactions and synergies were observed with respect to  $\text{CuO}/\text{La}_{0.5}\text{Sr}_{0.5}\text{CoO}_3$ . Sr-doping, in fact, enhances oxygen mobility affecting the reducing character of the nanodispersed CuO and thus the reactivity under different conditions [23].

The deposition of copper oxide significantly increases the activity of the nanocomposites in CO oxidation (about 100% conversion at 200°C) and in CO + NO (50% conversion at 250°C, more than 80% at 400°C) reactions. Comparing the nanocomposites obtained by depositing CuO clusters in undoped and Sr-doped lanthanum cobaltate, it is evident that the main difference concerns the compounds with lower Cu content. The catalysts obtained using the Sr-doped perovskite became highly active at lower temperature. On simulated gasoline engine exhaust, the nanocomposites always improve the oxidation activity compared to the parent perovskite, while the NO reduction is quantitative in the absence of  $\text{O}_2$ .

#### *3.1.4 From the powder to a functional device: the art of deposition*

Once the catalytic perovskite is developed and optimised from the compositional, morphological and structural point of view, the device realization is the next challenge. An interesting example is the deposition of the active layer onto a cordierite support, which is usually carried out in three-way catalysts systems. The traditional approach is rather time- and material-consuming, being composed by several steps of immersion in a perovskite suspension followed by heat treatments carried out slowly enough to avoid cracks in the active layer. With the aim of saving time and materials and thus to increase the sustainability of the catalytic system, we developed, starting from the Marcilly wet chemistry synthesis, an innovative procedure consisting in growing the perovskite directly on the cordierite honeycomb [24].

The cordierite support was immersed into a solution of precursors also containing the citric acid. A pH around 6–7 was obtained by adding drop to drop an aqueous solution of ammonia. The wet honeycomb was thus treated at the calcination temperature which is necessary to obtain the perovskite structure. In this way, the perovskite was grown directly on the support in a single step. Beside the time-saving, also the catalyst is required in lower amount and the cordierite surface is completely covered by the active perovskite. To evaluate this, the La/Si XPS atomic ratios as a function of weight increment have been reported (**Figure 4**). Fadley [25, 26] and Argile et al. [27], in fact, have shown that the atomic ratio between the XPS signals of supported and supporting species changes with the deposited amount in a different way for a homogeneous or a ‘island’ growth mechanism. The comparison with the literature data indicates, for the direct method, a deposition of a homogeneous layer and, for the washcoating procedure, the deposition by islands. This behaviour is also confirmed by SEM images (**Figures 5 and 6**). Moreover, the

amount of active layer deposited by direct procedure can be tuned by tuning the composition of the precursors' solution.

Finally, the porosity generated by gas evolution during the synthesis (comparing **Figures 5** and **6**) allows to reach a good surface area that contributes to increase the catalytic performance.

### 3.2 Cases of built functionality: carbon dioxide; from green-house-gas to synthetic fuel; and improvement of catalytic activity through exosolution

Methane dry reforming (MDR) is an endothermic reaction of high scientific and industrial importance that requires a very high temperature [28–31].

In spite of being studied from 1888, it is not yet considered an industrially mature process, mainly because of the C-poisoning and sintering of the catalysts which are based on noble metals or nickel. Several aspects affect the performances of catalyst: the strong interaction between supporting and active phases, the dispersion and size of active phase, the basicity, the reducibility, the oxygen exchange capability, porosity and specific surface area [29].

The mechanism of methane dry reforming has been investigated on several catalysts [32–34]. In general, four steps are considered: (1) dissociative adsorption of methane—which is the rate determining step and should be favoured by step active sites; (2) dissociative adsorption of  $\text{CO}_2$ —which is generally considered fast particularly on metal-support interface; (3) hydroxyl groups formation; and (4)

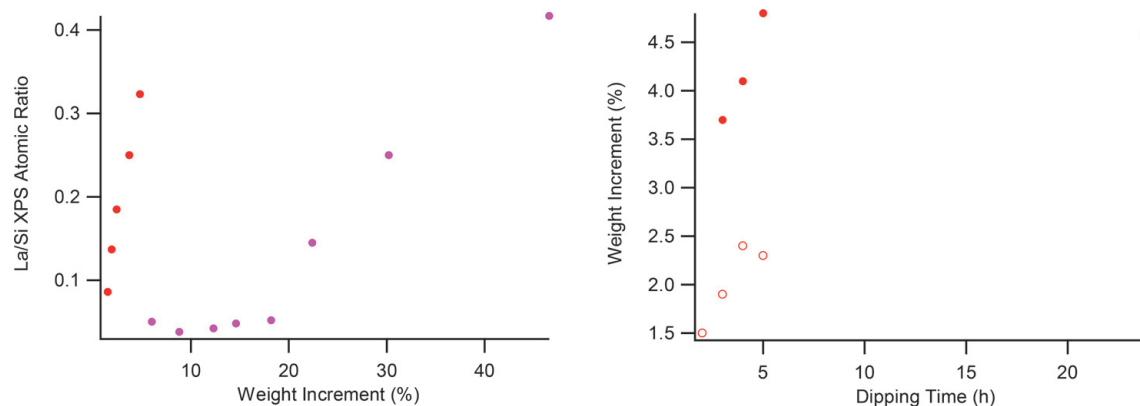


**Figure 4.** *La/Si atomic ratio (corresponding to the degree of coverage of the cordierite by  $\text{LaCoO}_3$ , being XPS a surface specific technique) observed in the direct (red) and washcoating (magenta) deposition procedures (left). Amount of catalyst deposited (evaluated by weight increment) with a solution of 12 g/l (filled circles) and 1.2 g/l (empty circles) of precursor (right).*

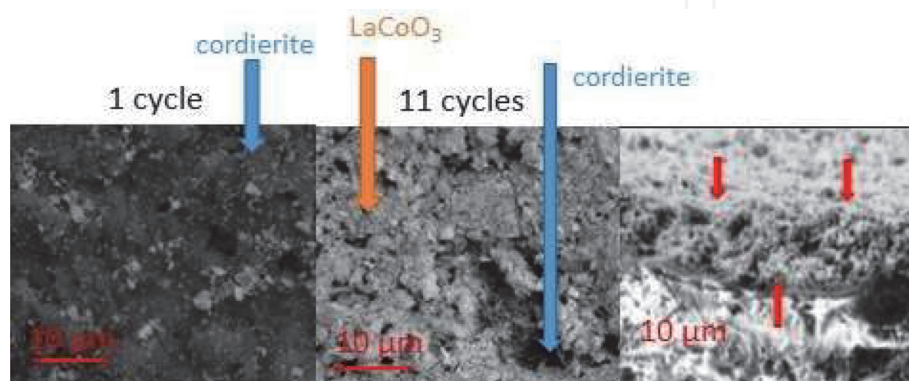


**Figure 5.** *SEM images of the cordierite surface during the increasing washcoating cycles and of the section.*



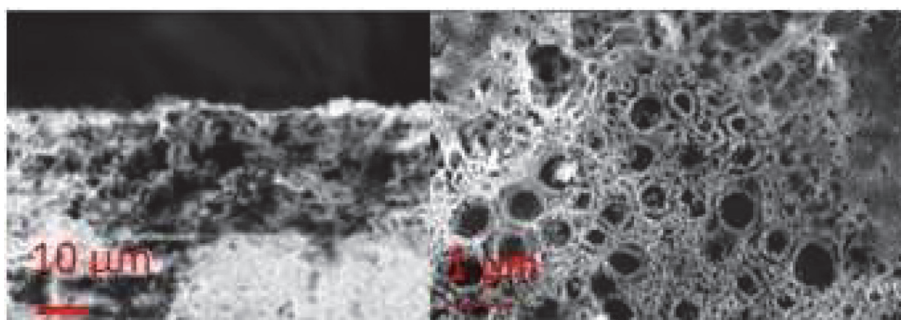


**Figure 6.** SEM images of the cordierite/LaCoO<sub>3</sub> section and surface after the deposition carried out by direct deposition.

intermediates oxidation and desorption—surface oxygen is considered responsible of the conversion of CH<sub>x</sub>–groups adsorbed on the surface in CO and H<sub>2</sub>. There is no consensus on the detailed reactions composing this last step but this can become a slow step depending on the specific support and catalyst.

Perovskites are frequently considered as a good strategy for improving the catalytic performance in MDR. In fact, there is a powerful technique capable of allowing the creation of highly dispersed and stabilized Ni clusters on the surface: exosolution [35]. Exosolution consists of a treatment of the perovskite (in this case, a Ni-containing perovskite) under reducing condition. This induces the Ni to exit from the perovskite cell and to migrate towards the surface creating a strong interaction with it. This strong interaction provides higher stability towards the Ni migration and sintering during reaction. Moreover, if lanthanum is present in the perovskite, a lanthanum oxycarbonate specie forms, preventing the C-poison.

To test the effect of copper doping into the activity of LaNiO<sub>3</sub>-based catalysts in MDR, we compared LaNiO<sub>3</sub> and LaNi<sub>0.7</sub>Cu<sub>0.3</sub>O<sub>3</sub>. Moreover, the nickelate has been modified by exosolution and by deposition of NiO nanoparticles.

The catalysts have been prepared by citrate route; the XRD patterns indicate that the crystalline phase is obtained after thermal treatment at 850°C; the BET specific surface area is 10–11 m<sup>2</sup>/g and is not affected by the insertion of copper.

Also the morphology is not really modified by the presence of copper (**Figure 7**).

The H<sub>2</sub> consumption determined in the TPR analysis indicates that in the LaNiO<sub>3</sub> sample, 17% of Ni is present as Ni(III), whereas in the Cu-doped, the % increases to 46%. This difference suggests that Cu increases the reducibility of Ni in the perovskite. This phenomenon, already observed for other perovskites, is attributed, following Tien-Taho et al. [36, 37], to the attitude of copper, under reducing conditions, to migrate towards the surface. Elemental copper distributed on the surface catalyses the H<sub>2</sub> activation decreasing the reduction temperatures. In fact, two reduction peaks are observed in the TPR curve of LaNiO<sub>3</sub>: one is centred at 434°C and is attributed to the Ni(III) to Ni(II) process, and the other at 595°C is due to the Ni(II) to Ni(0) reduction. When copper is inserted into the structure, the first peak (now corresponding to Ni(III) to Ni(II) and to Cu(II) to Cu(0) reductions) is shifted at 333°C and the second one at 566°C. XPS analysis allows to add some complementary and interesting information. Beside the peak shape and position, consistent with the presence of La(III) (see also the shake-up signal at 838 eV characteristic of this oxidation state for La—**Figure 8**) and Cu(II) (shake-up signal at 942–944 eV—**Figure 8**), it is evident that O 1s signal (**Figure 8**) is composed by two contributions attributed to perovskite lattice oxygen (528.8–529.0 eV) and to hydroxyl groups (531.7 eV). The quantitative analysis (**Table 8**) confirms the presence of surface contaminants (hydroxyl groups): the atomic percentage of oxygen is higher than the nominal one, particularly in the undoped sample. Lanthanum is surface segregated in

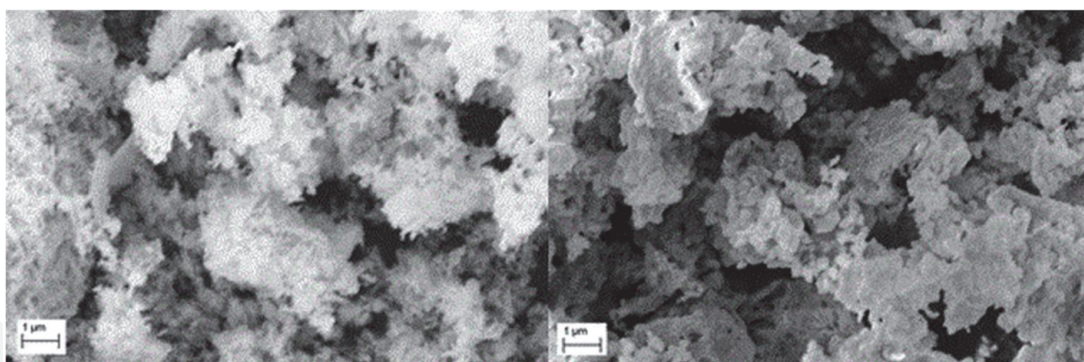


**Figure 7.**  
 SEM images obtained for the undoped (left) and Cu-doped (right)  $\text{LaNiO}_3$ .

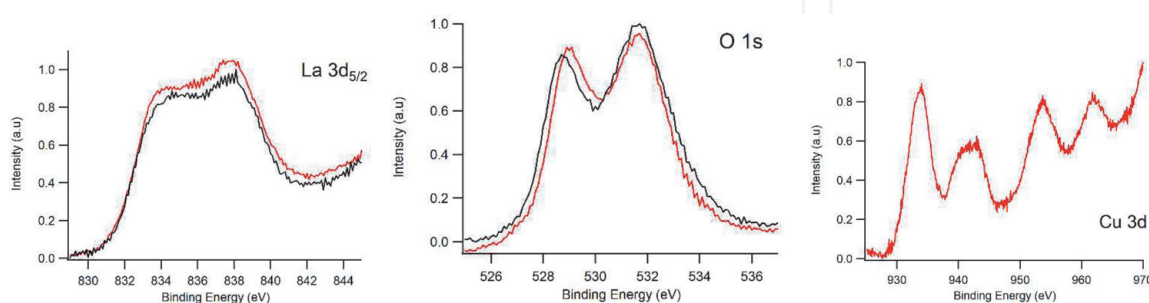


**Figure 8.**  
 XP spectra obtained for the undoped (black) and Cu-doped (red)  $\text{LaNiO}_3$ .

Sample		La	Ni	Cu	O	O/(La + Ni + Cu)	Cu/Ni
$\text{LaNiO}_3$	XPS	18.4	7.6		74.0	2.85	0.00
	Nominal	70.9	29.1		60.0	1.50	0.00
		20.0	20.0				
		50.0	50.0				
$\text{LaNi}_{0.7}\text{Cu}_{0.3}\text{O}_3$	XPS	15.3	4.6	13.8	66.3	1.97	3.00
	Nominal	45.5	13.6	40.9	60.0	1.50	0.43
		20.0	14.0	6.0			
		50.0	35.0	15.0			

**Table 8.**  
 Atomic composition obtained with XPS for the undoped and Cu-doped  $\text{LaNiO}_3$  compared with the nominal one determined by the weighted amounts.

the undoped sample but not in the doped one. In this case, it is evident that the copper is surface segregated (and this is expected to affect reactivity).

The reactivity of these doped and undoped nickelates is summarized in **Figure 9**.

No particularly evident differences can be observed between undoped and doped catalysts in spite of the relatively high amount of Cu inserted. A marked difference, by contrast, is evident by comparing the activity before and after the exosolution pretreatment (**Figure 10**). In this last case, in fact, the catalyst starts its activity at 600°C instead of 800°C.

### 3.3 Cases of built functionality: from catalysis to electrocatalysis; solid oxide fuel cells and solid oxide electrolysis cells

Beside catalyst-based systems, very important devices focusing on sustainable development are solid oxide fuel cells (SOFCs) and solid oxide electrolyzers (SOECs) [38, 39].

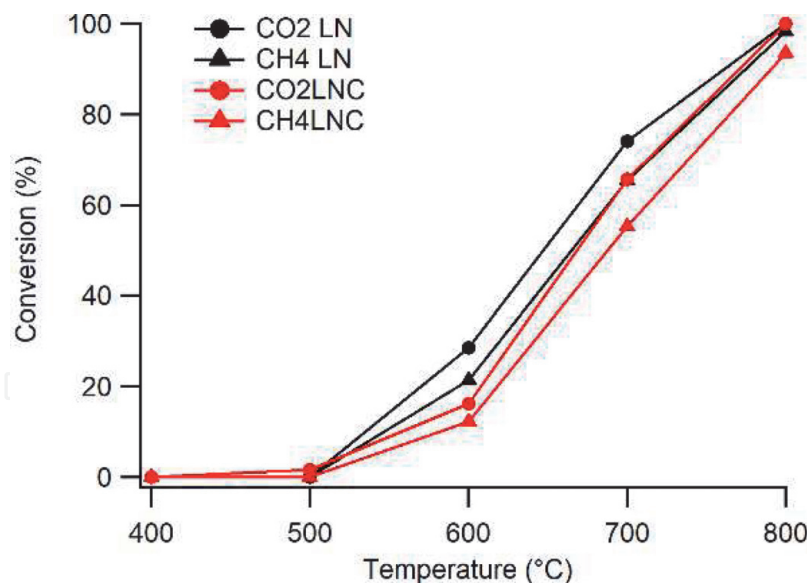


**Figure 9.**  $\text{CO}_2$  and  $\text{CH}_4$  conversion values obtained with undoped  $\text{LaNiO}_3$  (LN) and Cu-doped one (LNC).

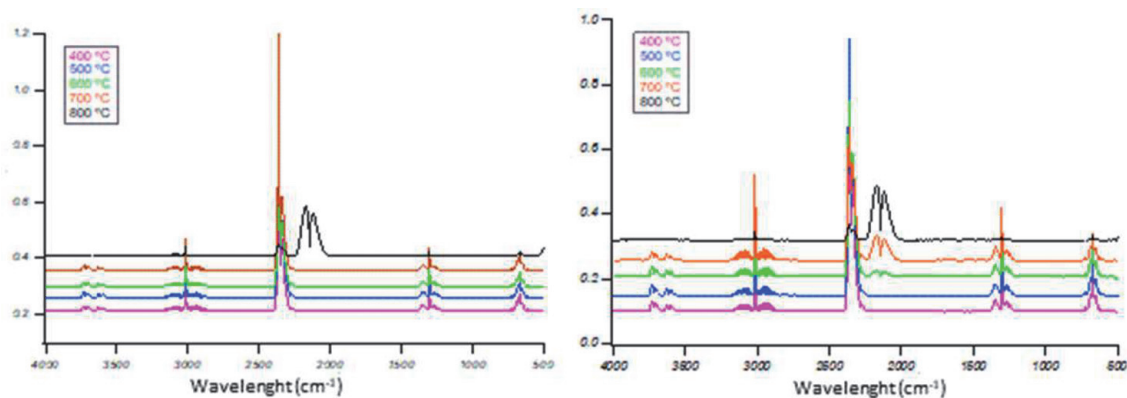


**Figure 10.** IR spectra obtained, as a function of temperature, upon exposure of the as-prepared (left) and exsoluted (right)  $\text{LaNiO}_3$  to  $\text{CO}_2 + \text{CH}_4$ .

SOFCs are electrochemical devices capable of converting the chemical energy of fuels into electrical energy; *vice versa* SOECs are devices that can convert the electric energy deriving, in excess, from intermittent renewable sources into the chemical energy of a fuel. Unlike other fuel cells, SOFCs operate at intermediate to high temperature (700–1000°C), and consequently, no noble metals are necessary to activate the electrodes. Another advantage is offered by the possibility to reverse the cell, that is, making it work as a fuel cell or as an electrolyser. This approach could be very advantageous because the endothermic requirements can be fulfilled by electric energy and temperature; moreover, the reversibility allows to minimise the problems related to the C-poisoning of the surface (when fuels different than pure hydrogen are used) and the electrode/electrolyte delamination. However, robust and durable materials are necessary due to the severe working conditions and, if reversible SOFCs are desired, the stability and catalytic activity are required both under oxidizing and reducing conditions. In our research group, we aim at developing reversible intermediate temperature (600–700°C) solid oxide fuel cells operating with C-containing fuels.

To reach this objective, we considered, at first, the starting point:  $(\text{La}, \text{Sr})(\text{Fe}, \text{Ga})\text{O}_3$  (LSGF). LSGF has only slightly lower performances with respect to the benchmark perovskite-based electrodes, but it exhibits an excellent chemical stability.



Strontium and gallium insertion enhances the oxygen mobility; in addition, gallium seems to enhance chemical stability in reducing conditions. Iron contributes to the electrochemical performances and also increases the electronic conductivity of the materials. Mixed ionic and electronic conductivity (MIEC) is a particularly important property for the electrodes in SOFCs. In fact, unlike traditional electronic conductors, MIEC allows to extend the active surface avoiding the problem of triple phase boundary (TPB). The composition exhibiting the best compromise between activity and stability has been identified in  $\text{La}_{0.6}\text{Sr}_{0.4}\text{Ga}_{0.3}\text{Fe}_{0.7}\text{O}_3$ ; hence, this is the starting point.

We have successfully synthesized  $\text{La}_{0.6}\text{Sr}_{0.4}\text{Ga}_{0.3}\text{Fe}_{0.7}\text{O}_3$  with a simple, controllable and easily scalable wet chemistry route: preparation with amounts from 0.5 to 15 g has been carried out and the obtained results demonstrated the high reproducibility of the method. We have investigated several parameters of the synthesis, setting the minimum amount of nitric acid at 4.5 ml per gram of product for a complete combustion, and the minimum calcination temperature at 900°C for a completely pure phase. The calcination temperature limits the superficial area, which is useful in particular for catalytic purposes, to 9 m<sup>2</sup>/g. Calcination temperature can be lowered if minor impurities are tolerated or whether the material will undergo cycles of reduction/oxidation. In this case, the perovskite auto-arranges towards the complete purity and the BET specific surface area is about twice. Investigations on the powders prior to calcination indicated that after the combustion, the perovskitic phase has already been formed, but persists a massive organic fraction that requires a temperature treatment for its removal. The resistance of the material to the reduction was tested between 800 and 1000°C, and the obtained results outline an exceptional resistance to reduction compared to the other perovskites: operation of the material in hydrogen atmospheres at 800°C leads only to minor structural modification. The resistance to reduction and the capability to recover the original structure after an oxidation treatment make this perovskite particularly suitable also for applications requiring tolerance to very reducing atmosphere. No differences of stability have been observed as a function of the different preparation conditions.

Once defined the starting point we considered necessary to improve the electrocatalytic activity. Also for this application, wet impregnation for nanocomposition was fundamental. To minimise the addition of complexity, we decided to create a nanocomposite of the type FeO<sub>x</sub>/LSGF for the cathode.

The use of nanocomposites powders as starting point for electrodes allows to deeply modify the electrochemical performance. A thin, Sr/Fe-rich foil forms on the surface of the electrode during the SOFC thermal treatment and deeply improves the electrochemical behaviour of the FeO<sub>x</sub>/LSGF cathode. The electrochemical results are encouraging for future application in SOFCs, as nanocomposite has an ASR of 2.1 Ω·cm<sup>2</sup> at 620°C, only 1/3 of LSGF's one in the same conditions.

### **3.4 Cases of built functionality: oxygen permeable dense ceramic membranes**

The efficiency of a fuel cell depends on (among other elements) the internal losses in the cell, including the ohmic resistance of the electrolyte and the overpotential losses at the electrodes. While the first one is well understood today, the second one needs a deeper characterisation. At the cathode site, in particular, the oxygen reduction is generally thought to be the most difficult reaction to activate in a SOFC. The mechanism appears rather elaborate and various aspects need to be considered [40, 41].

First, molecular O<sub>2</sub> needs to be converted into some 'electro-active' intermediate form via one or more processes. These reactions do not depend on the current



(except in the limit of steady state) and they are driven by the chemical potential (depletion or surplus of the intermediate). The second important point concerns the diffusion of the intermediate species (mass transfer) through the electrode (to the electrolyte). Since electrochemical reactions and diffusion occur cooperatively over an active area, the overall rate is co-limited by both these processes.

The oxygen permeation is a selective phenomenon that allows separating oxygen from a mixture of gases. **Figure 11** schematizes the permeation mechanism.

Oxygen undergoes reduction at the  $O_2$ -rich side, and then the oxide ions are transported through the membrane at the  $O_2$ -deficient side. The last step involves the re-oxidation of the oxide ions and the release of molecular oxygen. As can be seen, the driving force of the overall process is the  $O_2$  pressure gradient between the two sides of the membrane.

The permeation mechanism involves both the electrochemical and the transport properties of the investigated material.

It is now opportune to point out that the assumed mechanism can only be carried out by a MIEC. In fact, electrons must be able to move to the  $O_2$ -rich side to reduce  $O_2$ , and the oxide ions (generated at the oxygen-rich side) need to reach the  $O_2$ -deficient side.

The last feature involved in the permeation mechanism concerns the chemical properties of the material with respect to the reduction and oxidation of oxygen. From the statements above, a strong relationship between oxygen permeation properties and cathode activity is well evident: the processes involved in oxygen permeation and in SOFCs cathode working are very similar and the only difference concerns the last step (i.e. re-oxidation of oxide ions in the permeation process, compared to oxide ions transfer to the electrolyte in the SOFCs).

It should be evident that a high oxygen permeation rate can guarantee an overall fast operation when the material is employed as cathode in SOFCs.

The permeation phenomena can be described taking into account the oxygen ions and the electrons diffusion through the membrane. In detail, the working scheme summarized in **Figure 11** (left) suggests that electrons and ions move in opposite directions in order to give a total current density equal to zero under steady state conditions. Under these conditions, the oxygen flow,  $J_{O_2}$ , is strictly bound to the MIEC.

Doping can really increase the oxygen permeation both increasing the oxygen vacancies and mobility and surface reactivity, as evidenced by the  $J_{O_2}$  values obtained on  $LaCoO_3$  undoped and doped with Sr and with Cu (**Table 9**).

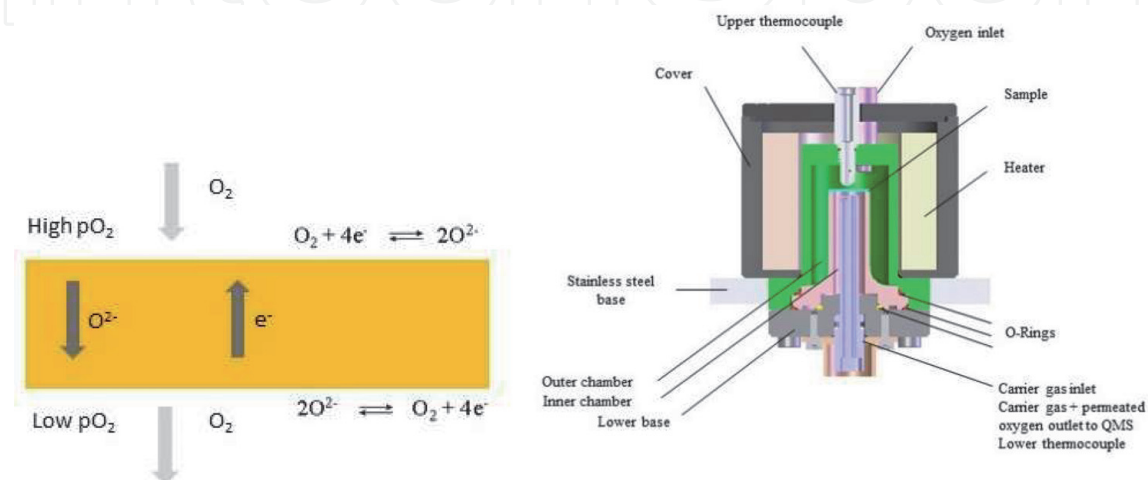


**Figure 11.** Schematic view of the oxygen permeation in a mixed electronic-ionic conductor (left) and of the device (right).

Sample	500	600	700
LaCoO <sub>3</sub>	0.7	0.7	0.8
LaCo <sub>0.5</sub> Cu <sub>0.5</sub> O <sub>3</sub>	1.6	1.5	1.6
La <sub>0.5</sub> Sr <sub>0.5</sub> Co <sub>0.5</sub> Cu <sub>0.5</sub> O <sub>3</sub>	0.8	1.0	1.3

**Table 9.** O<sub>2</sub> flow,  $JO_2 \times 10^{-2}$  mL/cm<sup>2</sup> min obtained as a function of temperature in undoped and doped LaCoO<sub>3</sub>.

## 4. Conclusions

Perovskites are versatile oxides whose properties can be tuned finely through different approaches. In this case, our focus is on ABO<sub>3</sub> perovskites. Among the relevant properties of oxide perovskites, we have considered catalysis and electrocatalysis. Both these fields are very interesting for sustainable development. Catalysis is relevant for abatement of pollutants (NO<sub>x</sub>, TWC, as an example) or for the production of green hydrogen and the conversion of carbon dioxide into fuel (dry reforming of methane); electrocatalysis is the basis for the realization of solid oxide cells (fuel cells and electrolyzers). Several aspects are fundamental both for catalysis and electrocatalysis, such as the presence of active sites on the surface of the perovskites or the development of oxygen mobility and exchange.

To develop these properties in perovskites, there are several possibilities: in this contribution, we underline the opportunities offered by doping, nanocomposition and exosolution.

Several perovskites of the type LaCoO<sub>3</sub>, SrTiO<sub>3</sub>, LaMnO<sub>3</sub> and LaFeO<sub>3</sub> have been considered and the effect of doping in the A-site (Sr, K) and B-site (Cu, Mn, Co) has been evaluated.

When a complex functionality is required, nanocomposition is sometimes preferred. Nanocomposition can be carried out by different procedures. In this contribution, the materials have been obtained by wet impregnation, a traditional procedure, and by ammonia driven precipitation, an innovative method that, based on the use of complexants, allows obtaining highly dispersed particles. Several composites of the type CuO<sub>x</sub>/Perovskite (LaCoO<sub>3</sub>, (La,Sr)CoO<sub>3</sub>, LaNiO<sub>3</sub> and SrTi<sub>0.7</sub>Co<sub>0.3</sub>O<sub>3</sub>) have been investigated and compared. The catalytic activity depends on the interaction between the deposited active phase and the support, and on the exchange properties of the system.

A further complexity characterises electrocatalysts: beside the catalytic attitude, the conductivity is fundamental. In our research, the focus is on the development of electrodes for SOFCs and SOECs (the fuel and air electrodes). To this purpose, an important improvement is constituted by the simultaneous presence of ionic and electronic conductivity (mixed ionic electronic conductivity—MIEC). In MIEC electrodes, the reactions extend over the whole surface, whereas in the purely electronic conductors, it is possible only at the interphase between electrode/electrolyte reached by gas phase reactants (triple boundary zone). One of the bottlenecks to the commercialization of solid oxide cell is due to the cost and durability. Both these aspects are connected to the high-operating temperature (800–1000°C). So, beside MIEC, it is very important to decrease the operating temperature approaching intermediate temperature. Finally, to go further, it is useful to be able to use C-containing fuels that can be derived from biogas, natural gas, etc. In our research, we developed several electrodes active at 600–700°C in solid oxide fuel cells and solid oxide electrolysis cells. To assure stability, we also considered very robust perovskites of the type SrTiO<sub>3</sub> or La<sub>1-x</sub>Sr<sub>x</sub>Ga<sub>1-y</sub>Fe<sub>y</sub>O<sub>3</sub>, increasing their performance by doping, nanocomposition and infiltration.

By means of these strategies, we obtained performant electrodes and, moreover, in some cases, electrodes for reversible solid oxide cells. Reversible cells can operate both as SOFCs and as SOECs and, finally, can behave as super-batteries for energy storage.

The oxygen mobility added to the activity in oxidation and in reduction can make perovskites good candidate for the realization of dense ceramic membranes for the separation of gases. We studied, as an example, the effect of doping on the permeability to O<sub>2</sub> of LaCoO<sub>3</sub>-based perovskites.

In this contribution, our aim was in demonstrating that, by means of doping, nanocomposition and exsolution, we can create highly active catalysts and electrocatalysts. This was also shown considering the dry reforming of methane, a very important reaction capable of converting greenhouse gases into fuel (syngas). Without the use of noble or costly metals, we developed sustainable doped SrTiO<sub>3</sub> active in DRM at 650–700°C.

Also the conversion of a powder into device has been considered focusing on the case of three-way catalysts. An innovative procedure for the ‘deposition’ of the active perovskite phase on cordierite was developed and the obtained results have been compared to those obtained by means of the traditional washcoating procedure: both catalysts and time waste are avoided and an efficient system is obtained by direct deposition.

## **Acknowledgements**

The research leading to these results has received funding from the European Union’s H2020 Programme under grant agreement 686086 PARTIAL-PGMs.

## **Conflict of interest**

The authors declare no conflict of interest.

## **Author details**


Andrea Bedon<sup>1</sup> and Antonella Glisenti<sup>2\*</sup>

1 Efesto Innovation, Padova, Italy

2 Department of Chemical Sciences, University of Padova, Italy

\*Address all correspondence to: [antonella.glisenti@unipd.it](mailto:antonella.glisenti@unipd.it)

## **IntechOpen**

© 2020 The Author(s). Licensee IntechOpen. This chapter is distributed under the terms of the Creative Commons Attribution License (<http://creativecommons.org/licenses/by/3.0>), which permits unrestricted use, distribution, and reproduction in any medium, provided the original work is properly cited. 

## References

- [1] Peña MA, Fierro JLG. Chemical structures and performance of perovskite oxides. *Chemical Reviews*. 2001;**101**: 1981-2017. DOI: 10.1021/cr980129f
- [2] Marcilly C, Courty P, Delmon B. *Journal of the American Ceramic Society*. 1970;**53**:56-57. DOI: 10.1111/j.1151-2916.1970.tb12003.x
- [3] Schwarz JA, Contescu C, Contescu A. Methods for preparation of catalytic materials. *Chemical Reviews*. 1995;**95**: 477-510. DOI: 10.1021/cr00035a002
- [4] Kung HH. *Transition Metal Oxides: Surface Chemistry and Catalysis – Studies in Surface Science and Catalysis*. Vol. 45. Elsevier Science Publishers; 1989
- [5] Guiotto M, Pacella M, Perin G, Iovino A, Michelon N, Natile MM, et al. *Applied Catalysis A: General*. 2015;**499**: 146-157. DOI: 10.1016/j.apcata.2015.04.013
- [6] Mul G, Neeft JPA, Kapteijn F, Makkee M, Moulijn JA. *Applied Catalysis B: Environmental*. 1995;**6**: 339-352
- [7] Glisenti A, Natile MM, Carlotto S, Vittadini A. Co- and Cu-doped titanates: Toward a new generation of catalytic converters. *Catalysis Letters*. 2014;**144**: 1466-1471. DOI: 10.1007/s10562-014-1294-5
- [8] Carlotto S, Natile MM, Glisenti A, Vittadini A. Electronic structure of  $\text{SrTi}_{1-x}\text{M}_x\text{O}_{3-\delta}$  (M = Co, Ni, Cu) perovskite-type doped titanate crystals by DFT and DFT plus U calculations. *Chemical Physics Letters*. 2013;**588**: 102-108. DOI: 10.1016/j.cplett.2013.10.020
- [9] Carlotto S, Natile MM, Glisenti A, Vittadini A. Adsorption of small molecules at the cobalt-doped  $\text{SrTiO}_3(001)$  surface: A first-principles investigation. *Surface Science*. 2015;**633**: 68-76. DOI: 10.1016/j.susc.2014.11.025
- [10] Carlotto S, Natile MM, Glisenti A, Vittadini A. Adsorption of CO and formation of carbonates at steps of pure and Codoped  $\text{SrTiO}_3$  surfaces by DFT calculations. *Applied Surface Science*. 2016;**364**:522-527. DOI: 10.1016/j.apsusc.2015.12.194
- [11] Carlotto S, Natile MM, Glisenti A, Paul J-F, Blanck D, Vittadini A. Energetics of CO oxidation on lanthanide-free perovskite systems: The case of Co-doped  $\text{SrTiO}_3$ . *Physical Chemistry Chemical Physics*. 2016;**18**: 33282-33286. DOI: 10.1039/c6cp03994d
- [12] Carlotto S, Natile MM, Glisenti A, Vittadini A. Catalytic mechanisms of NO reduction in a CO-NO atmosphere at Co- and Cu-doped  $\text{SrTiO}_3(100)$  surfaces. *Journal of Physical Chemistry C*. 2018;**122**:449-454. DOI: 10.1021/acs.jpcc.7b09279
- [13] DeZanet A, Peron G, Natile MM, Vittadini A, Glisenti A. Synthesis and development of four way catalysts starting from critical raw material free Perovskites: Influence of doping and synthesis conditions. *Topics in Catalysis*. 2019;**62**:237-243. DOI: 10.1007/s11244-018-1119-7
- [14] Glisenti A, Pacella M, Guiotto M, Natile MM, Canu P. Largely Cu-doped  $\text{LaCo}_{1-x}\text{Cu}_x\text{O}_3$  perovskites for TWC: Toward new PGM-free catalysts. *Applied Catalysis B: Environmental*. 2016;**180**:94-105. DOI: 10.1016/j.apcatb.2015.06.017
- [15] Pacella M, Garbujo A, Fabro J, Guiotto M, Xin Q, Natile MM, et al. PGM-free  $\text{CuO/LaCoO}_3$  nanocomposites: New opportunities for TWC application. *Applied Catalysis B:*



- Environmental. 2018;**227**:446-458. DOI: 10.1016/j.apcatb.2018.01.053
- [16] Grillo F, Natile MM, Glisenti A. Low temperature oxidation of carbon monoxide: The influence of water and oxygen on the reactivity of a  $\text{Co}_3\text{O}_4$  powder surface. *Applied Catalysis B: Environmental*. 2004;**48**:267-274. DOI: 10.1016/j.apcatb.2003.11.003
- [17] Garbujo A, Pacella M, Natile MM, Guiotto M, Fabro J, Canu P, et al. On A-doping strategy for tuning the TWC catalytic performance of perovskite based catalysts. *Applied Catalysis A: General*. 2017;**544**:94-107. DOI: 10.1016/j.apcata.2017.07.009
- [18] Pinto D, Glisenti A. Pulsed reactivity on  $\text{LaCoO}_3$ -based perovskites: A comprehensive approach to go inside CO oxidation mechanism and the effect of dopants. *Catalysis Science & Technology*. 2019;**9**:2749-2757. DOI: 10.1039/C9CY00210C
- [19] Glisenti A, Galenda A, Natile MM.  $\text{La}_{0.7}\text{Sr}_{0.3}\text{CuO}_{3-\delta}$ : An interesting catalyst for methanol and ethanol treatment. *Catalysis Letters*. 2013;**143**:254-259. DOI: 10.1007/s10562-012-0954-6
- [20] Glisenti A, Galenda A, Natile MM. Steam reforming and oxidative steam reforming of methanol and ethanol: The behaviour of  $\text{LaCo}_{0.7}\text{Cu}_{0.3}\text{O}_3$ . *Applied Catalysis A: General*. 2013;**453**:102-112. DOI: 10.1016/j.apcata.2012.11.031
- [21] Perin G, Fabro J, Guiotto M, Xin Q, Natile MM, Cool P, et al.  $\text{Cu@LaNiO}_3$  based nanocomposites in TWC applications. *Applied Catalysis B: Environmental*. 2017;**209**:214-227. DOI: 10.1016/j.apcatb.2017.02.064
- [22] Somorjai GA. *Introduction to Surface Chemistry and Catalysis*. New York: John Wiley & Sons Inc;
- [23] Carollo G, Garbujo A, Xin Q, Fabro J, Cool P, Canu P, et al.  $\text{CuO}/\text{La}_{0.5}\text{Sr}_{0.5}\text{CoO}_3$  nanocomposites in TWC reference: APCATB\_117753. *Applied Catalysis B: Environmental*. in press
- [24] Guiotto M, Pacella M, Perin G, Iovino A, Michelon N, Natile MM, et al. Washcoating vs. direct synthesis of  $\text{LaCoO}_3$  on monoliths for environmental applications. *Applied Catalysis A: General*. 2015;**499**:146-157. DOI: 10.1016/j.apcata.2015.04.013
- [25] Fadley CS. Angle-resolved X-ray photoelectron spectroscopy. *Progress in Surface Science*. 1984;**16**:275-388. DOI: 10.1016/0079-6816(84)90001-7
- [26] Fadley CS. *Basic Concepts of X-Ray Photoelectron Spectroscopy in Electron Spectroscopy: Theory, Techniques and Application*. Vol. 2. London: Academic Press; 1978
- [27] Argile C, Rhead GE. Adsorbed layer and thin film growth modes monitored by Auger electron spectroscopy. *Surface Science Reports*. 1989;**30**:277-356. DOI: 10.1016/0167-5729(89)90001-0
- [28] Pakhare D, Spivey J. A review of dry ( $\text{CO}_2$ ) reforming of methane over noble metal catalysts. *Chemical Society Reviews*. 2014;**43**:7813-7837. DOI: 10.1039/c3cs60395d
- [29] Jang WJ, Shim J-O, Kim H-M, Yoo S-Y, Roh H-S. A review on dry reforming of methane in aspect of catalytic properties. *Catalysis Today*. 2019;**324**:15-26. DOI: 10.1016/j.cattod.2018.07.032
- [30] Wang Y, Yao L, Wang S, Mao D, Hu C. Low-temperature catalytic  $\text{CO}_2$  dry reforming of methane on Ni-based catalysts: A review. *Fuel Processing Technology*. 2018;**169**:199-206. DOI: 10.1016/j.fuproc.2017.10.007
- [31] Aramouni NAK, Touma JG, Tarboush BA, Zeaiter J, Ahmad MN. Catalyst design for dry reforming of methane: Analysis review. *Renewable*

- and Sustainable Energy Reviews. 2018; **82**:2570-2585. DOI: 10.1016/j.rser.2017.09.076
- [32] Papadopoulou C, Matralis H, Verykios X. Utilization of biogas as a renewable carbon source: Dry reforming of methane. In: *Catalysis for Alternative Energy Generation*. New York: Springer. pp. 57-127
- [33] Kumar N, Kanitkar S, Wang Z, Haynes D, Shekhawat D, Spivey JJ. Dry reforming of methane with isotopic gas mixture over Ni-based pyrochlore catalyst. *International Journal of Hydrogen Energy*. 2019, 2019;**44**: 4167-4176. DOI: 10.1016/j.ijhydene.2018.12.145
- [34] Bachiller-Baeza B, Mateos-Pedrero C, Soria MA, Guerrero-Ruiz A, Rodemerck U, Rodríguez-Ramos I. Transient studies of low-temperature dry reforming of methane over Ni-CaO/ZrO<sub>2</sub>-La<sub>2</sub>O<sub>3</sub>. *Applied Catalysis B: Environmental*. 2013;**129**:450-459. DOI: 10.1016/j.apcatb.2012.09.052
- [35] Ye LT, Zhang MY, Huang P, Guo GC, Hong MC, Li CS, et al. Enhancing CO<sub>2</sub> electrolysis through synergistic control of non-stoichiometry and doping to tune cathode surface structures. *Nature Communications*. 2017;**8**:14785. DOI: 10.1038/ncomms14785
- [36] Tien-Thao N, Alamdari H, Zahedi-Niaki MH, Kaliaguine S. *Applied Catalysis A: General*. 2006;**311**:204-212. DOI: 10.1016/j.apcata.2006.06.029
- [37] Tien Thao N, Alamdari H, Kaliaguine S. *Journal of Solid State Chemistry*. 2008;**181**:2006-2019. DOI: 10.1016/j.jssc.2007.11.016
- [38] Bedon A, Natile MM, Glisenti A. On the synthesis and stability of La<sub>0.6</sub>Sr<sub>0.4</sub>Ga<sub>0.3</sub>Fe<sub>0.7</sub>O<sub>3</sub>. *Journal of the European Ceramic Society*. 2017;**37**: 1049-1058. DOI: 10.1016/j.jeurceramsoc.2016.10.017
- [39] Bedon A, Rieu M, Viricelle JP, Glisenti A. Rational development of IT-SOFC electrodes based on the Nanofunctionalization of La<sub>0.6</sub>Sr<sub>0.4</sub>Ga<sub>0.3</sub>Fe<sub>0.7</sub>O<sub>3</sub> with oxides. PART 1: Cathodes by means of Iron oxide. *ACS Applied Energy Materials*. 2018;**1**:6840-6850. DOI: 10.1021/acsaem.8b01124
- [40] Galenda A, Natile MM, Glisenti A. Oxygen permeation measurements: An alternative tool to select new intermediate temperature solid oxide fuel cell cathodes. *Nanoscience and Nanotechnology Letters*. 2011;**3**:723-730. DOI: 10.1166/nnl.2011.1227
- [41] Natile MM, Eger G, Batocchi P, Mauvy F, Glisenti A. Strontium and copper doped LaCoO<sub>3</sub>: New cathode materials for solid oxide fuel cells? *International Journal of Hydrogen Energy*. 2017;**42**:1724-1735. DOI: 10.1016/j.ijhydene.2016.09.127